TABLE I

Measured values of dielectric constant at 10 GHz

Material	Measured dielectric constant by 1-thickness method*		Measured dielectric constant by 2-thickness method	Available dielectric constant
	d=b/4	d= b/2		
Benzene (20°C)	1.47	1.79	2.27	2.285[4] (at 20°C and 9.4 GHz)
Cyclohexane (20°C)	1.43	1.66	2.04	2.024 [4] (at 20°C and 9.4 GHz)
Perspex	2.46	2.55	2.61	2.60 [5] (at 5.0 GHz)

* One thickness results are only for comparison.

the slotted waveguide such that the required thickness of the dielectric layer is obtained. The guide wavelength is measured for two thicknesses with the help of the probe in the slot and the standing wave ratio (SWR) meter. Knowing the frequency, the two thicknesses, and the corresponding wavelengths, the dielectric constant is evaluated using (13). Some of the results are given in Table I. Values of the dielectric constant are also calculated using (1)–(3) for two thicknesses separately and reported in the same table.

Discussion

The experimental values of the dielectric constants of benzene, cyclohexane, and Perspex, obtained by using the two thickness formulation, are in good agreement with the corresponding available values in the literature. The formulation in the proposed method does not require any quasi-static approximation which is needed in the cavity perturbation method. Also in the present method the problem of mode jumping does not exist. However, the propagation of higher order modes in such an H-plane loaded waveguide [2] can be avoided by careful selection of two thicknesses of the dielectric material. For example, $\epsilon_r \leq 2.66$ and $f \leq 10$ GHz, higher order modes do not propagate for $d \leq b/2$. Our results indicate that the one thickness method fails to give agreeable values of ϵ_r. It seems that there is some experimental error in the one thickness method and it gets cancelled when the two thickness method is used. The other advantage of this two thickness method is that (11) and (12) can be solved both graphically and numerically, while for the one thickness method no convenient graphical method is available. In order to make this method more practicable, tables for ϵ_r can be made for various combinations of λ_{g1} and λ_{g2}. Also the proposed method does not require a sophisticated sample holder used in other methods. It uses commonly available slotted waveguide, but the use is restricted to noncorrosive materials.

The results obtained for liquids and solids are accurate to within 0.8 percent of the values available in the literature. The guide wavelength and the thickness of the dielectric slab are normally measured to the accuracy of 0.005 cm, and an error of this magnitude corresponds to less than 1 percent in ϵ_r.

Acknowledgment

The authors wish to thank Prof. K. C. Gupta for helpful discussions and suggestions.

References

[1] I. J. Bahl and K. C. Gupta, "Measurement of parameters of an artificial dielectric using a partially filled parallel plate waveguide," *Int. J. Electron.*, vol. 28, pp. 173–177, Feb. 1970.
[2] F. Gardiol and A. Vander Vorst, "Wave propagation in a rectangular waveguide loaded with an H-plane dielectric slab," *IEEE Trans. Microwave Theory Tech.*, MTT-17, pp. 56–57, Jan. 1969.
[3] N. Marcuvitz, *Waveguide Handbook* (M.I.T. Rad. Lab. Series), vol. 10. New York: McGraw-Hill, 1951, p. 392.
[4] B. Bleaney, F. H. N. Loubser, and R. P. Penrose, "Cavity resonators for measurements with centimeter electromagnetic waves," *Proc. Phys. Soc. (London)*, vol. 59, p. 196, Mar. 1947.
[5] S. Roberts and A. Von Hippel, "A new method of measuring dielectric constant and loss in the range of centimetre waves," *J. Appl. Phys.*, vol. 17, p. 616, July 1946.

A Finite Difference Method for the Solution of Electromagnetic Waveguide Discontinuity Problems

G. MUR

***Abstract*—A finite difference method for the numerical solution of electromagnetic waveguide discontinuity problems is presented. The method of boundary relaxation is applied, using finite difference techniques in the nonuniform section of the waveguide and using a modal representation of the field in the uniform sections of the waveguide.**

To illustrate the process some two-dimensional diffraction problems in an electromagnetic waveguide with rectangular cross section are solved.

I. Introduction

Finite difference methods for the numerical solution of boundary value problems are limited to problems involving only relatively small regions, due to limitations on computer time and storage requirements. Applying the method of "boundary relaxation," Silvester and Cermak [1]–[3], Richter [4], and Sandy and Sage [5] have been able to reduce considerably the number of mesh points required and thus have reduced computing time and storage problems. The method of boundary relaxation involves the choice of an appropriate artificial boundary that limits the region to which the finite difference scheme is applied.

In this short paper an alternative method to determine the field distribution on the artificial boundary is described. Contrary to the method indicated above, it does not require the computation and storage of a large matrix and is therefore, in general, less storage and time consuming. The artificial boundary in our configuration is chosen such that the field in a suitably chosen exterior region can easily be expressed in terms of some type of modal representation of the wave function. To illustrate the process we solve some two-dimensional diffraction problems in an electromagnetic waveguide with rectangular cross section. The modal representation of the field in the exterior domain has also been used by Patwari and Davies [6] in their computation of the field scattered by conducting cylinders. However, they did not employ boundary relaxation, but used a direct method to solve the relevant system of equations.

II. Formulation of the Problem

As an example illustrating our version of the technique of boundary relaxation, we determine the scattering properties of a cylindrical obstacle and/or a cylindrical wall deformation present in a finite section of an otherwise uniform electromagnetic waveguide with rectangular cross section. To locate a point in the configuration, a right-handed Cartesian coordinate system x,y,z is introduced. The z axis is chosen parallel to the axis of the waveguide; the y axis is taken parallel to the direction of cylindricity of the obstacle and/or the wall deformation. The waveguide walls and the obstacle are assumed to be electrically perfectly conducting. The medium inside the waveguide is linear, homogeneous, isotropic, and lossless; its electromagnetic properties are characterized by a permittivity ϵ and a permeability μ. The analysis is carried out in terms of LSE and LSM fields [7], [8]. As the obstacle and/or the deformed waveguide walls are uniform in the y-direction, the total field will show the same y-dependence as the prescribed incident field. Furthermore, no coupling between LSE and LSM fields takes place.

A longitudinal cross section of the configuration to be investigated is shown in Fig. 1. The nonuniformity of the waveguide is assumed to be located in the region between the reference planes $z = z_1$ and $z = z_2$. All field quantities are assumed to vary sinusoidally in time with angular frequency ω. The complex time factor $\exp(i\omega t)$ is omitted in the formulas.

An LSE field is an electromagnetic field in the configuration for which $E_y = 0$ and $H_y \not\equiv 0$. H_y can be written as

$$H_y = \Psi(x,z) \sin(n\pi y/b), \qquad (n = 1,2,\cdots) \tag{1}$$

Manuscript received January 11, 1973; revised July 2, 1973.
The author is with the Department of Electrical Engineering, Division of Electromagnetic Research, Delft University of Technology, Delft, The Netherlands.

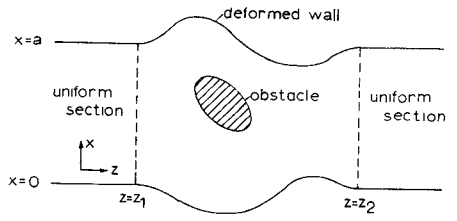

Fig. 1. Cross section of a rectangular waveguide with a cylindrical obstacle and cylindrically deformed walls.

where b is the internal dimension of the structure in the y-direction. In the uniform sections $-\infty < z < z_1$ and $z_2 < z < \infty$ of the waveguide (see Fig. 1), the LSE field can be expressed in terms of LSE modes which are defined as

$$\Psi_m^{\pm} \overset{\text{def}}{=} \cos(m\pi x/a)\exp(\mp\gamma_m z), \qquad (m = 0,1,2,\cdots) \tag{2}$$

with

$$\gamma_m \overset{\text{def}}{=} [(m\pi/a)^2 - \kappa^2]^{1/2} \text{ with } \operatorname{Re}(\gamma_m) \geq 0, \qquad \operatorname{Im}(\gamma_m) \geq 0 \tag{3}$$

and

$$\kappa \overset{\text{def}}{=} [\omega^2\epsilon\mu - (n\pi/b)^2]^{1/2}. \tag{4}$$

In (2) the upper signs represent modes that are either traveling or decaying exponentially in the positive z-direction, and the lower signs represent modes that are either traveling or decaying exponentially in the negative z-direction. On the waveguide walls and on the boundary surface of the obstacle the boundary condition $(\partial/\partial n)\Psi = 0$ holds, where $(\partial/\partial n)$ denotes the directional derivative along the normal to the boundary.

An LSM field is an electromagnetic field in the configuration for which $E_y \not\equiv 0$ and $H_y = 0$. E_y can be written as

$$E_y = \Phi(x,z)\cos(n\pi y/b), \qquad (n = 0,1,2,\cdots). \tag{5}$$

In the uniform sections of the waveguide the LSM field can be expressed in terms of LSM modes which are defined as

$$\Phi_m^{\pm} \overset{\text{def}}{=} \sin(m\pi x/a)\exp(\mp\gamma_m z), \qquad (m = 1,2,\cdots) \tag{6}$$

where γ_m is given by (3). On the waveguide walls and on the boundary surface of the obstacle the boundary condition $\Phi = 0$ holds. At any interior point of the configuration the wave functions Ψ and Φ satisfy the two-dimensional Helmholtz equation

$$\left(\frac{\partial^2}{\partial x^2} + \frac{\partial^2}{\partial z^2} + \kappa^2\right)\{\Psi,\Phi\} = 0. \tag{7}$$

In view of the difference in handling the field quantities in the exterior domain $-\infty < z < z_1$ and $z_2 < z < \infty$, i.e., in the uniform sections outside the reference planes, and in the interior domain $z_1 < z < z_2$ containing the obstacle and/or wall deformations, we distinguish an exterior and an interior problem.

A. Exterior Problem

In the uniform sections $-\infty < z < z_1$ and $z_2 < z < \infty$ the electromagnetic fields can be written as a superposition of waveguide modes. In the region $-\infty < z < z_1$ the electromagnetic field consists of a single incident mode Ψ_N^+ or Φ_N^+ traveling in the positive z-direction and a reflected field consisting of a superposition of modes that are either traveling or decaying exponentially in the negative z-direction. The modal expansion in this region is written as

$$\Psi = \Psi_N^+ + \sum_{m=0}^{\infty} R_m\Psi_m^-, \qquad \text{for LSE fields}$$

$$\Phi = \Phi_N^+ + \sum_{m=1}^{\infty} \rho_m\Phi_m^-, \qquad \text{for LSM fields.} \tag{8}$$

In these expressions R_m and ρ_m denote the reflection factor for the mth mode.

In the region $z_2 < z < \infty$ the field consists of a superposition of transmitted modes that are either traveling or decaying exponentially in the positive z-direction. Hence

$$\Psi = \sum_{m=0}^{\infty} T_m\Psi_m^+, \qquad \text{for LSE fields}$$

$$\Phi = \sum_{m=1}^{\infty} \tau_m\Phi_m^+, \qquad \text{for LSM fields.} \tag{9}$$

In these expressions T_m and τ_m denote the transmission factor for the mth mode.

B. Interior Problem

In connection with the computation of the field in the region where the wall is deformed and/or the obstacles are present, we cover the longitudinal waveguide cross section between the planes $z = z_1 - h$ and $z = z_2 + h$ with a square mesh of side length h, where h is chosen such that $a = N_1h$ and $z_2 - z_1 = N_2h$, where N_1 and N_2 are positive integers. The reason for extending the mesh into the regions where the modal expansions hold, is that in that case the reflection and transmission factors can be determined numerically from values of the field at internal points of the mesh located in the uniform sections of the waveguide. In the interior region $z_1 - h < z < z_2 + h$, the Helmholtz equation (7) is approximated by the difference equation

$$\phi(x,z) = \frac{\phi(x+h,z) + \phi(x-h,z) + \phi(x,z+h) + \phi(x,z-h)}{4 - \kappa^2h^2} \tag{10}$$

where $\phi(x,z)$ denotes the value of either Ψ or Φ at a node of the mesh with the coordinates (x,z). The error in (10) is of order $0(h^2)$. In the LSE case we have, in addition to (7), the boundary condition $(\partial/\partial n)\Psi = 0$. In the LSM case we have the boundary condition $\Phi = 0$. An interpolation of degree zero [9], [10] is applied to approximate these boundary conditions.

III. Solution of the Problem

The iteration scheme to solve the problem in the *LSE case* proceeds as follows.

a) A starting value of both the field at the nodes of the mesh and of the reflection and transmission factors is chosen.

b) The field values at the nodes in the planes $z = z_1 - h$ and $z = z_2 + h$ are computed from the reflection and transmission factors. In this respect we have [cf. (8) and (9)].

$$\Psi(nh,z_1 - h) = \Psi_N^+(nh,z_1 - h) + \sum_{m=0}^{M} R_m\Psi_m^-(nh,z_1 - h), \qquad \text{with } n = 0,1,\cdots,N_1 \tag{11}$$

$$\Psi(nh,z_2 + h) = \sum_{m=0}^{M} T_m\Psi_m^+(nh,z_2 + h) \tag{12}$$

in which $M + 1$ is the number of modes taken into account.

c) New estimates for the field value at the nodes in the interior region are computed using the method of point successive overrelaxation [11]. The $(\nu + 1)$th estimate of the field value $\phi^{(\nu+1)}(x,z)$ then satisfies the equation

$$\phi^{(\nu+1)}(x,z) = \omega(4 - \kappa^2h^2)^{-1}(\phi^{(\nu+1)}(x-h,z) + \phi^{(\nu)}(x+h,z) + \phi^{(\nu+1)}(x,z-h) + \phi^{(\nu)}(x,z+h)) + (1-\omega)\phi^{(\nu)}(x,z) \tag{13}$$

where ω is the so-called relaxation factor (not to be confused with the angular frequency introduced earlier). The optimum value of this factor is difficult to determine, but $\omega = 1.7$ turns out to yield an adequate acceleration in the iteration scheme in many problems we have investigated. Configurations with a small interior region

and the use of a relatively coarse mesh, however, require a lower value of ω.

d) New estimates of the reflection and transmission factors are computed from the field values at the planes $z = z_1$ and $z = z_2$. At these planes the modal expansion holds. Hence, at the plane $z = z_1$ we have

$$\sum_{m=0}^{M} R_m \Psi_m^-(x,z_1) = \Psi(x,z_1) - \Psi_N^+(x,z_1). \tag{14}$$

The right-hand side of (14) is known at the $N_1 + 1$ points $x = nh$, $z = z_1$ with $n = 0,1,\cdots,N_1$. A Fourier cosine series can be constructed [cf. (2)] up to $N_1 + 1$ terms from the field values at these $N_1 + 1$ nodes, although a lower number of terms will be used in the actual numerical process (in practice M is much less than $N_1 + 1$, e.g., $M = 5$ and $N_1 = 30$). From the coefficients of this series the new estimates of the reflection factors can be determined easily upon using (14) and (2). At the plane $z = z_2$ we have

$$\sum_{m=0}^{M} T_m \Psi_m^+(x,z_2) = \Psi(x,z_2). \tag{15}$$

A Fourier cosine series [cf. (2)] can be constructed up to $N_1 + 1$ terms. The number of terms used is the same as in (14). From the coefficients of this series new estimates of the transmission factors can be determined upon using (15) and (2). Also a relaxation procedure, but with complex relaxation factor, is applied to the determination of the reflection and transmission factors. Let $\sigma^{(\nu)}$ denote the current estimate of either a reflection or a transmission factor and let $\sigma^{(\nu+1)'}$ denote the new estimate obtained as described above, then we use

$$\sigma^{(\nu+1)} = \Omega\sigma^{(\nu+1)'} + (1 - \Omega)\sigma^{(\nu)} \tag{16}$$

as the new estimate for this factor, where Ω denotes the complex relaxation factor for the reflection and transmission factors. The process converges with

$$\Omega = -\alpha i \,|\, 1 - \gamma_m h \,|/(1 - \gamma_m h) \tag{17}$$

when σ pertains to a propagating mode and with

$$\Omega = \alpha \tag{18}$$

when σ pertains to an exponentially decaying mode. In (17) and (18) α is a positive real number. The optimum value of α, which is dependent on the value of the relaxation factor occurring in (13), has to be determined experimentally: $\alpha = 1.25$ turns out to yield an adequate acceleration.

e) If the process has not yet converged to a final value, we return to b).

The iteration scheme to solve the problem in the *LSM case* is essentially the same as the iteration scheme in the LSE case. The optimum values of α and of the relaxation factor ω are approximately the same as those in the LSE case.

Since during the process no large matrices are introduced, it is obvious that the storage requirements of this method are determined mainly by the storage requirements of the field distribution at the nodes and not by the so-called "shift matrix" as used by Silvester and Cermak [3] and others. This holds even when the field distribution matrix and the shift matrix are overlayed, since the largest storage requirement is posed by the shift matrix [3].

On the same grounds, our method is computationally faster. We do need a matrix in order to store the transverse field distribution of the modes. This matrix requires the storage of $M \times (N_1 + 1)$ real numbers [i.e., $\cos(m\pi nh/a)$ and $\sin(m\pi nh/a)$ at $m = 1,2,\cdots,M$ and $n = 0,1,\cdots,N_1$ (cf. (11) and (12))], and it can easily be computed and requires a negligible amount of storage. Further, using the shift matrix the number of multiplications in order to compute a new estimate of the field value on the boundaries $z = z_1 - h$ or $z = z_2 + h$ is approximately N_1^2. Using our method, however, this number of multiplications is $2 \times M \times N_1 + 0(M)$, this number being connected with the computations in the steps c) and d). It is much less than N_1^2 and makes the process accordingly faster.

The process in solving the interior problem will be divergent as soon as κ^2h^2 has a value which is either equal to or greater than the first eigenvalue λ_1 of the homogeneous Dirichlet problem associated with the interior region. This is caused by the fact that the coefficient matrix B associated with our system of finite difference equations is no longer positive definite, which is necessary for convergence. The iteration process can again be made convergent by positive definiting [9], i.e., by multiplying the system of equations by the transpose B^T of B. Now, the matrix $C = B^TB$ is positive definite as long as $\kappa^2h^2 \neq \lambda_n$, where λ_n is the nth eigenvalue of the homogeneous Dirichlet problem. C becomes singular at $\kappa^2h^2 = \lambda_n$ and the system of equations cannot be solved. This difficulty can, in principle, be avoided by slightly displacing the artificial boundaries; this leaves the physical problem unchanged, but alters slightly the values of λ_n.

The convergence of the method of positive definite successive overrelaxation, however, has turned out to be poor even with optimally chosen relaxation factors. In order to accelerate this convergence we have constructed an analog of the alternating direction implicit (ADI) method developed by Conte and Dames [12] for the biharmonic equation. The corresponding result, however, still converges rather poorly, especially when $\kappa^2h^2 \simeq \lambda_n$, $n = 1,2,\cdots$. Therefore, in the following section numerical results will only be given for problems with $\kappa^2h^2 < \lambda_1$.

IV. Numerical Results

As an example illustrating the technique described in Section III, we compute the reflection and the transmission factors of a thick diaphragm as well as the reflection factor of several combinations of two triangularly prismatic wall deformations. As the incident wave we take the dominant $TE_{0,1}$ mode in a waveguide of rectangular cross section. The dimensions of the waveguide are chosen to satisfy the standardized relation $b = 2a$ in the LSE case and $a = 2b$ in the LSM case.

A. Thick Diaphragm

A symmetrical diaphragm of width equal to $0.25a$ has been chosen. In Figs. 2 and 3 the modulus and the argument of the reflection and the transmission factors are presented for an incident $LSE_{0,1}$ and $LSM_{1,0}$ mode, respectively. The frequency F of the incident field is chosen to be 1.3, 1.5, and 1.7 times the cutoff frequency FC of the dominant mode in the waveguide. The results are shown as a function of d ($a - 2d$ = gap width of the diaphragm).

B. Triangularly Prismatic Wall Deformation

Three different combinations of triangularly prismatic wall deformations have been considered. The longitudinal cross section of the wall deformations has the form of a right-angled isosceles triangle, deforming the waveguide wall either inwardly or outwardly. The height of either triangle is taken to be $0.1a$. Two of these deformations are placed opposite to each other in three different combinations: a) inward–inward; b) inward–outward; and c) outward–outward. In both the LSE and the LSM case the modulus of the reflection factor is shown as a function of the frequency in Fig. 4. The overall computing time for obtaining a single value of the reflection and transmission factors for the configurations shown in Figs. 2, 3, and 4 amounts to 15 s in the LSE case and to 5 s in the LSM case. The resulting accuracy is better than a few percent which was satisfactory for our purposes. The accuracy of the result can easily be improved by continuing the iterative process further and, if necessary, by choosing a finer mesh. Because of the fast convergence we can use the norm of the displacement vector, i.e., the norm of the difference between two successive solutions, as a measure for the error. Also the use of the norm of the displacement of the reflection and transmission factors only turned out to yield good results. The advantage of the latter method is that the computation of the latter norm hardly requires any computation time at all. The computations have been performed on the IBM 360/65 computer of the Computing Center of the Delft University of Technology.

Acknowledgment

The author wishes to thank Prof. A. T. de Hoop for his suggestions and remarks concerning the research presented in this short paper.

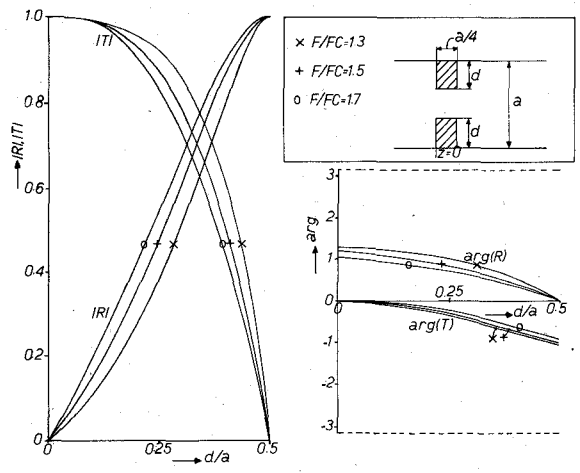

Fig. 2. Reflection and transmission factor of a thick diaphragm (incident $LSE_{0,1}$ mode = dominant mode).

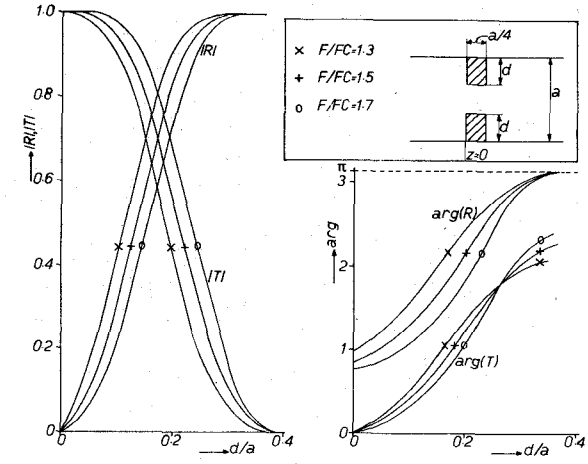

Fig. 3. Reflection and transmission factor of a thick diaphragm (incident $LSM_{1,0}$ mode = dominant mode). When $0.4 < d/a < 0.5$, $|T|$ is negligibly small.

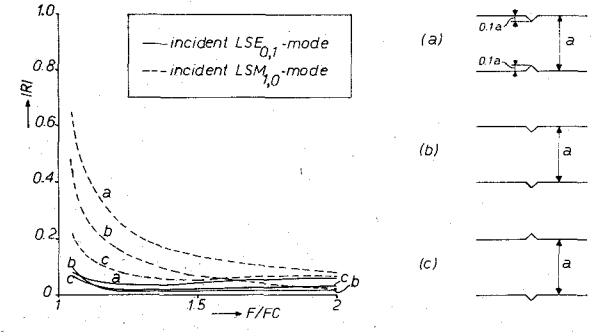

Fig. 4. Reflection factor of triangularly prismatic wall deformations in a rectangular waveguide.

References

[1] I. A. Cermak and P. Silvester, "Solution of two-dimensional field problems by boundary relaxation," *Proc. Inst. Elec. Eng. (London)*, vol. 115, pp. 1341–1348, 1968.

[2] P. Silvester and I. A. Cermak, "Analysis of coaxial line discontinuities by boundary relaxation," *IEEE Trans. Microwave Theory Tech. (Special Issue on Computer-Oriented Microwave Practices)*, vol. MTT-17, pp. 489–495, Aug. 1969.

[3] I. A. Cermak and P. Silvester, "Boundary-relaxation analysis of rotationally symmetric electric field problems," *IEEE Trans. Power App. Syst.*, vol. PAS-89, pp. 925–932, May/June 1970.

[4] S. L. Richter, "Extension of boundary relaxation for finite-difference solution of field problems," *Proc. IEEE* (Lett.), vol. 58, pp. 1146–1148, July 1970.

[5] F. Sandy and J. Sage, "Use of finite difference approximations to partial differential equations for problems having boundaries at infinity," *IEEE Trans. Microwave Theory Tech.* (Corresp.), vol. MTT-19, pp. 484–486, May 1971.

[6] A. M. Patwari and J. B. Davies, "Scattering by infinite cylinders of arbitrary cross-section by the method of finite differences," *Electron. Lett.*, vol. 2, pp. 470–471, Dec. 1966.

[7] R. E. Collin, *Field Theory of Guided Waves*. New York: McGraw-Hill, 1960, pp. 225–229.

[8] G. De Jong, "Scattering by a perfectly conducting cylindrical obstacle in a rectangular waveguide," *Int. J. Electron.*, vol. 32, pp. 153–167, 1972.

[9] M. J. Beaubien and A. Wexler, "An accurate finite-difference method for higher order waveguide modes," *IEEE Trans. Microwave Theory Tech. (1968 Symposium Issue)*, vol. MTT-16, pp. 1007–1017, Dec. 1968.

[10] G. E. Forsythe and W. R. Wasow, *Finite Difference Methods for Partial Differential Equations*. New York: Wiley, 1960, p. 198.

[11] R. S. Varga, *Matrix Iterative Analysis*. Englewood Cliffs, N.J.: Prentice-Hall, 1962, p. 59.

[12] S. D. Conte and R. T. Dames, "An alternating direction method for solving the biharmonic equation," *Math. Tables Other Aids Comput.*, vol. 12, pp. 198–205, 1958.

Finite-Gap Stripline-Latching Circulator

M. E. EL-SHANDWILY, MEMBER, IEEE, AND ESMAT A. F. ABDALLAH, STUDENT MEMBER, IEEE

***Abstract*—The stripline-latching circulator with finite gap is analyzed theoretically. The normalized resonant frequencies of the first-order modes and the normalized circulation frequencies are obtained numerically for different values of the gapwidth and dielectric constant of the ceramic filling the nonmagnetic gap.**

I. Introduction

Recently, Siekanowicz and Schilling [1] presented a theory for a three-port stripline-latching ferrite-junction circulator. The operation of the circulator is achieved by passing a pulse of direct current through a wire loop which is located between a ferrite cylinder and a concentric ferrite ring. The upper and lower portions of the ferrite ring and rod are in contact with ferrite disks. The circulator is switched by reversing the polarity of the current pulse.

The analysis of Siekanowicz and Schilling is an extension of Bosma's [2] and Fay and Comstock's [3] analyses for the stripline circulator. However, the effect of the nonmagnetic gap, in which the wire loop is located, has not been taken into consideration. In this short paper, we present the theory of the stripline-latching circulator with finite-nonmagnetic gap. The effect of the gapwidth and dielectric material on the circulator performance will be investigated.

II. Analysis

The configuration of the stripline-latching circulator is shown in Fig. 1 [1]. In the following analysis, the circulator junction is divided into three regions; the ferrite post ($0 \le r \le r_1$), the nonmagnetic gap ($r_1 \le r \le r_2$), and the outer ferrite ring ($r_2 \le r \le r_3$). The electric fields in the three regions are

$$E_z^{\mathrm{I}} = J_n(x)\,(a_n e^{jn\phi} + a_{-n} e^{-jn\phi}), \qquad 0 \le r \le r_1 \tag{1}$$

$$E_z^{\mathrm{II}} = J_n(y)\,(b_n e^{jn\phi} + b_{-n} e^{-jn\phi}) + Y_n(y)\,(C_n e^{jn\phi} + C_{-n} e^{-jn\phi}), \qquad r_1 \le r \le r_2 \tag{2}$$

$$E_z^{\mathrm{III}} = J_n(x)\,(d_n e^{jn\phi} + d_{-n} e^{-jn\phi}) + Y_n(x)\,(f_n e^{jn\phi} + f_{-n} e^{-jn\phi}), \qquad r_2 \le r \le r_3 \tag{3}$$

Manuscript received February 5, 1973; revised June 22, 1973.
The authors are with the Electrical and Electronic Engineering Laboratory, National Research Centre, Dokki, Cairo, Egypt.